Supporting Information

Controlling Electron Transport towards Efficient All-Solution-Processed Quantum Dot Light Emitting Diodes

Hongting Chen[a,b,†], Ke Ding[b,†], Lianwei Fan[b], Rui Zhang[b], Runda Guo[b], Jibin Zhang[a,b], Lintao Hou[a,*] and Lei Wang[b,*]

[a]Guangzhou Key Laboratory of Vacuum Coating Technologies and New Energy Materials, Siyuan Laboratory, Department of Physics, Jinan University, Guangzhou 510632, China
[b]Wuhan National Laboratory for Optoelectronics, Huazhong University of Science and Technology, Wuhan 430074, China
* Correspondence author: thlt@jnu.edu.cn; wanglei@mail.hust.edu.cn
[†]These authors contributed equally to the work.

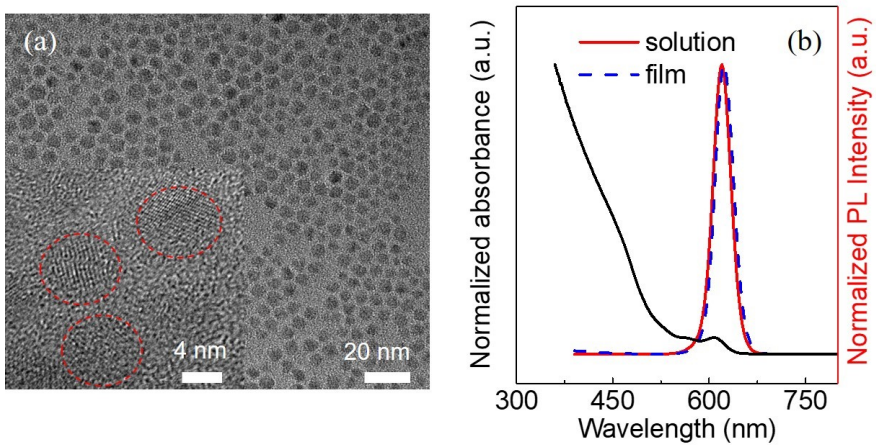

Figure S1. (a) TEM images of CdSe/CdS/ZnS QDs, the inset is the related HRTEM image. (b) Ultraviolet-visible absorption and PL spectra of QDs. The black solid line represents for absorption in toluene. The red solid line represents for PL in toluene and the blue dashed line represents for the PL spectrum in solid state.

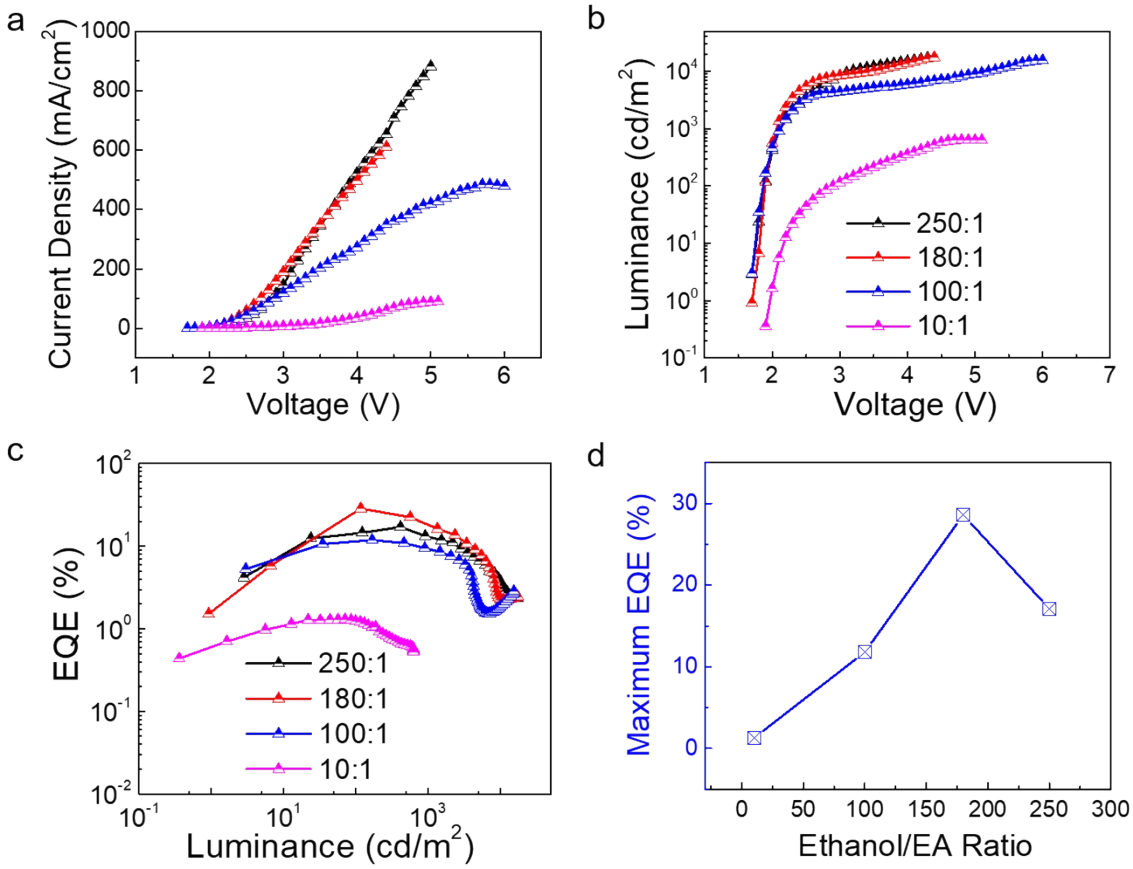

Figure S2. Comparison of the device performance for QLED based on ZnO with different EA-doping ratios. (a, b) Current density and luminance characteristics as a function of bias voltage. (c) EQE characteristics as a function of luminance. (d) The maximum EQE versus different doping ratios of EA.

Table S1. Performance of QLEDs based on ZnO NPs with different EA-doping ratios.

Devices	EL peak (nm)	V_T[a)] (V)	Max. Lu[b)] (cd m^{-2})	Max. EQE (%)	Max. CE (cd A^{-2})	Max. PE (lm W^{-2})
250:1	632	1.75	17210	17.1	19.5	30.6
180:1	632	1.75	17490	28.6	31.6	52.3
100:1	632	1.75	15450	11.8	13.3	22.1
10:1	624	2.0	631	1.29	1.85	2.52

[a)]V_T is the turn on voltage. [b)]Max. Lu is the maximum luminance.

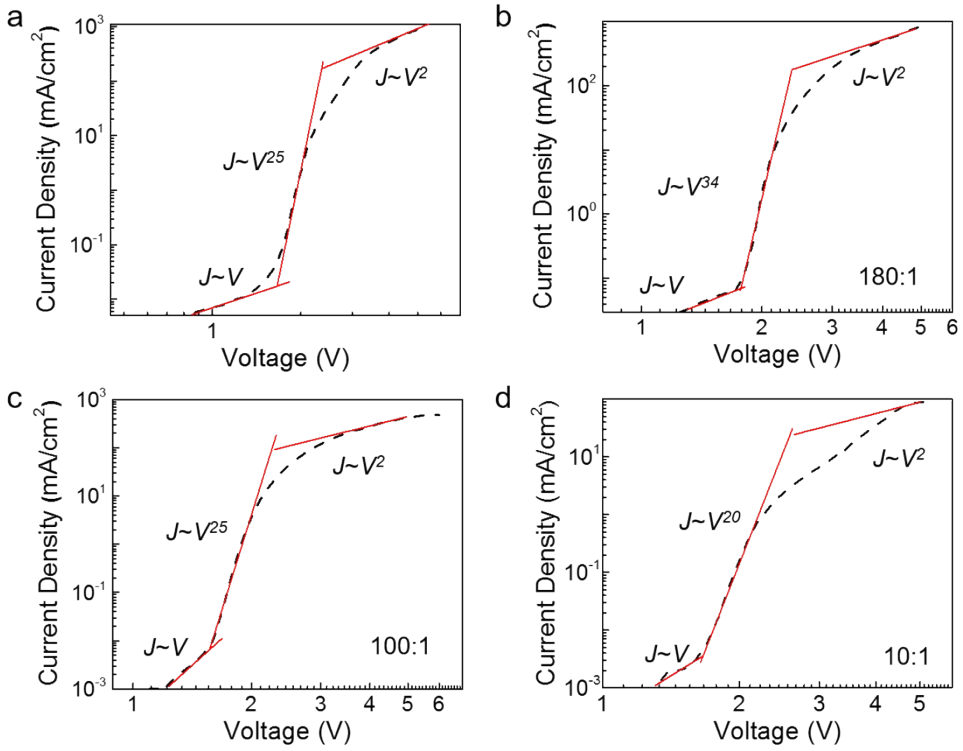

Figure S3. Current density-voltage curves and the corresponding fitting plots of ZnO NPs based QLEDs with different EA-doping ratios. (a) 250:1. (b) 180:1. (c) 100:1. (d) 10:1.

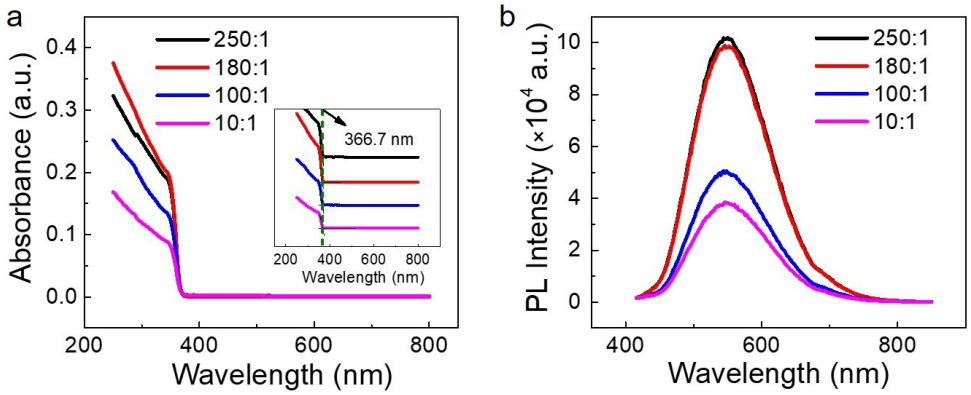

Figure S4. The ultraviolet-visible absorption and PL spectra of ZnO NPs in ethanol with different EA-doping ratio. (a) The UV-visible absorption spectra. The inset is the enlarged view of the peak. (b) The PL spectra with the excited wavelength of 365 nm.

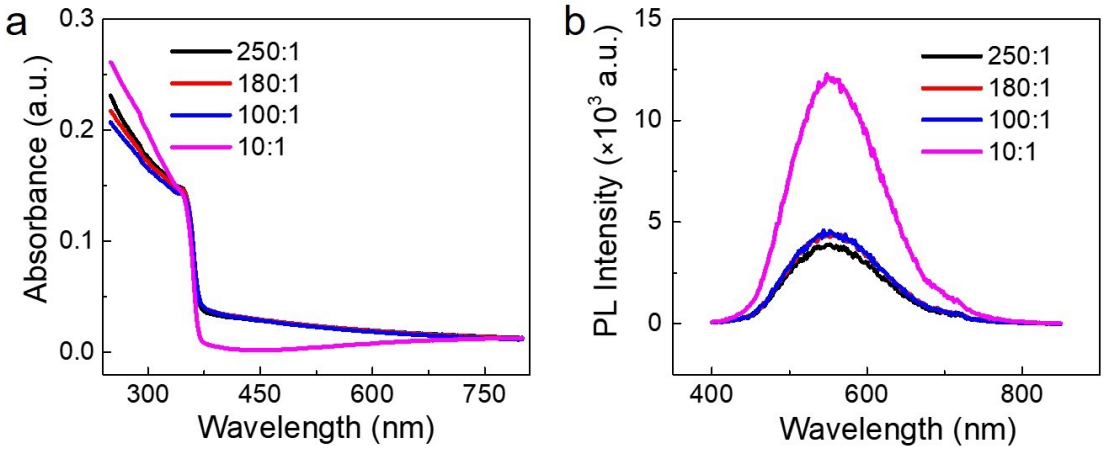

Figure S5. The ultraviolet-visible absorption and PL spectra of ZnO NPs films with different EA-doping ratios. (a) The UV-visible absorption spectra. (b) The PL spectra with the excited wavelength of 365 nm.

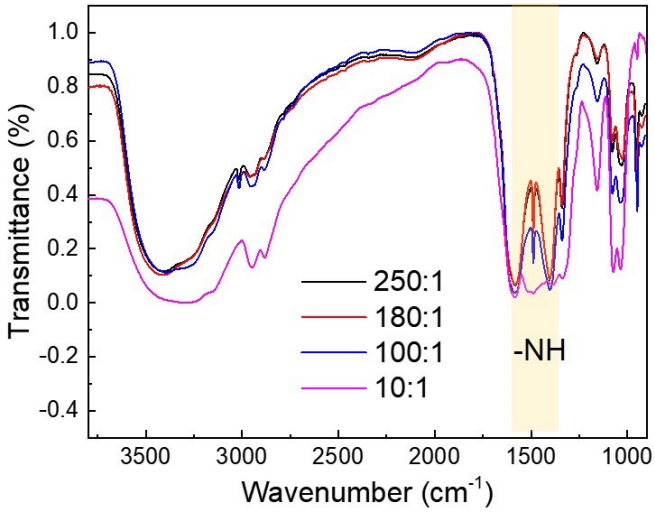

Figure S6. The FTIR spectra of the ZnO NPs films with different EA-doping ratio.

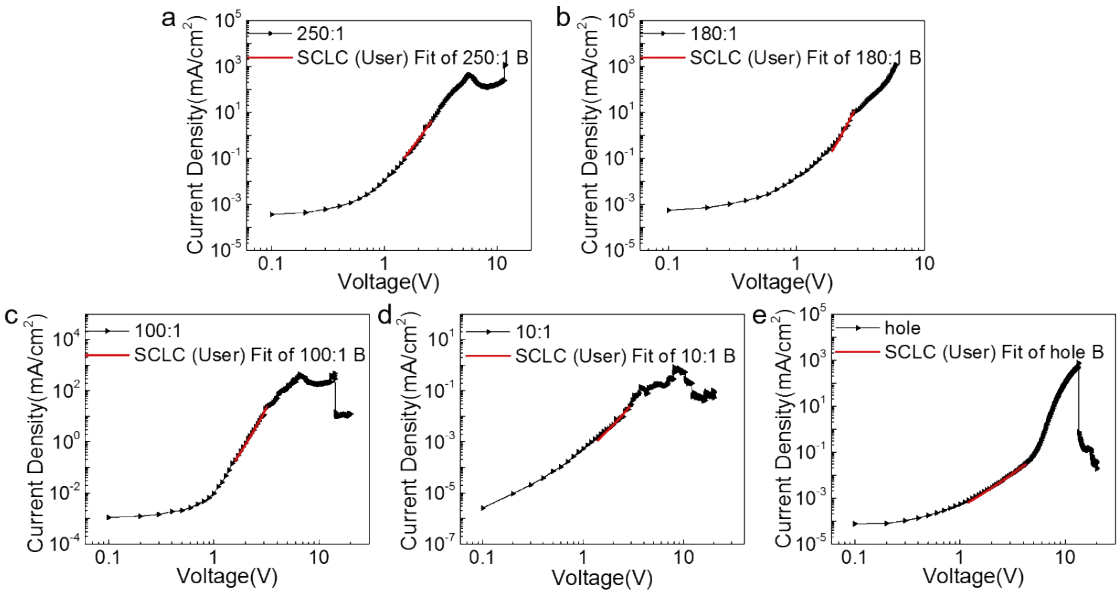

Figure S7. The SCLC fitting for the current density-voltage curves of hole-only device and electron-only devices based on ZnO NPs with different EA-doping ratios. (a) 250:1. (b) 180:1. (c) 100:1. (d) 10:1. (e) hole-only device.

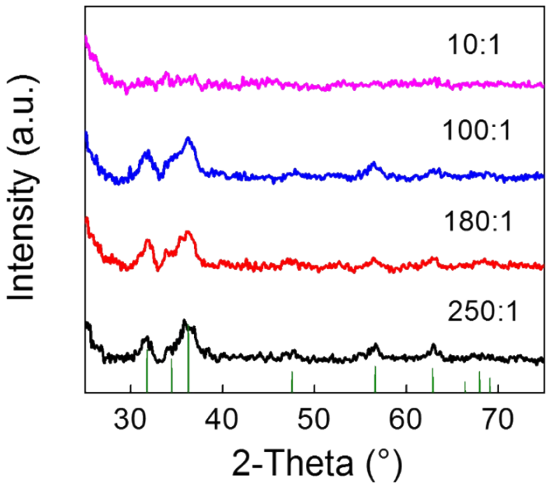

Figure S8. The XRD patterns of the films of ZnO NPs with different EA-doping ratios.

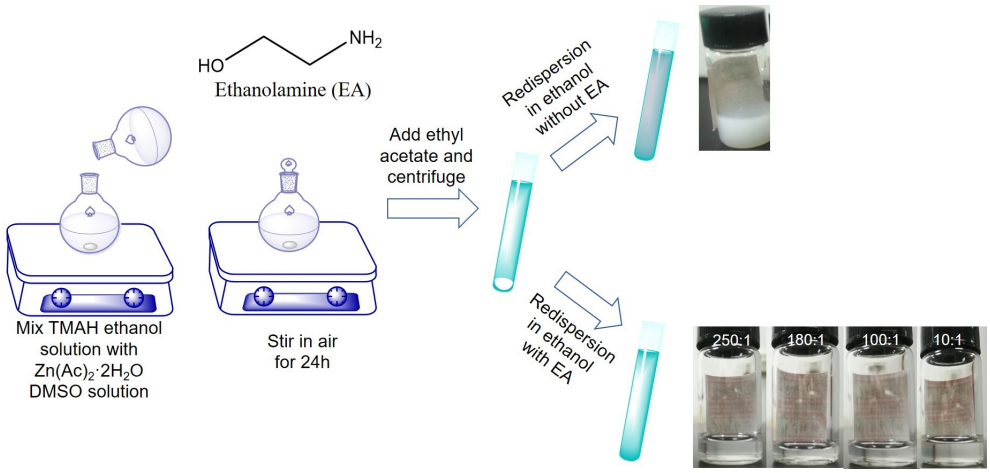

Figure S9. The preparation process of ZnO NPs with and without EA.

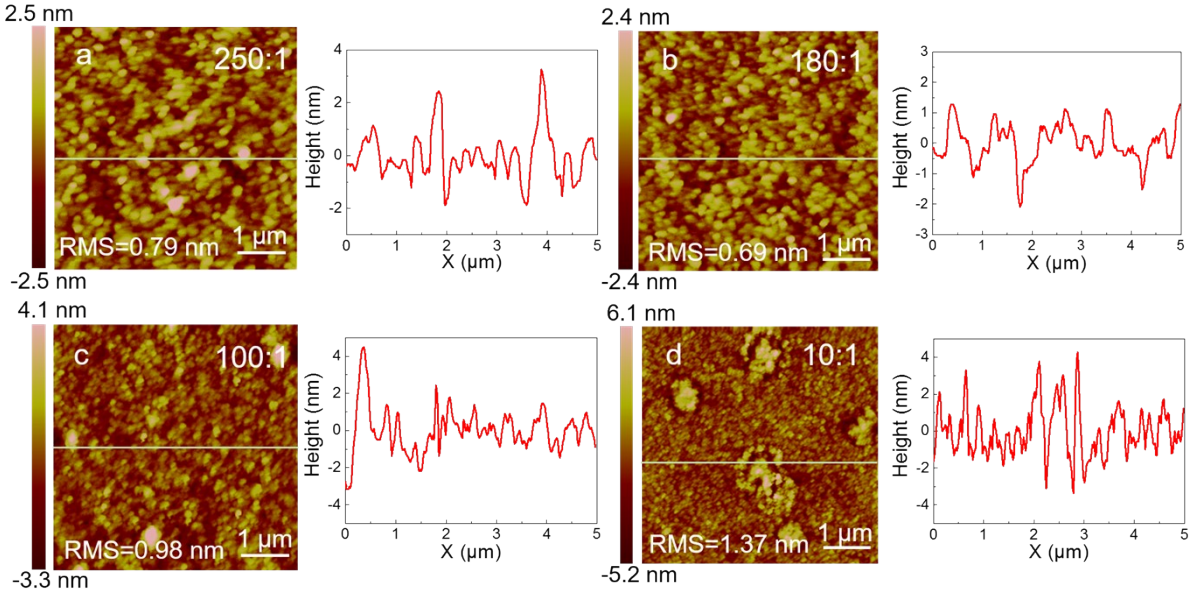

Figure S10. The AFM images and the corresponding line-scan profiles of ZnO NPs films with different EA-doping ratios on the substrate of the multilayer of ITO/PEDOT:PSS/poly-TPD/PVK/QDs. (a) 250:1. (b) 180:1. (c) 100:1. (d) 10:1.

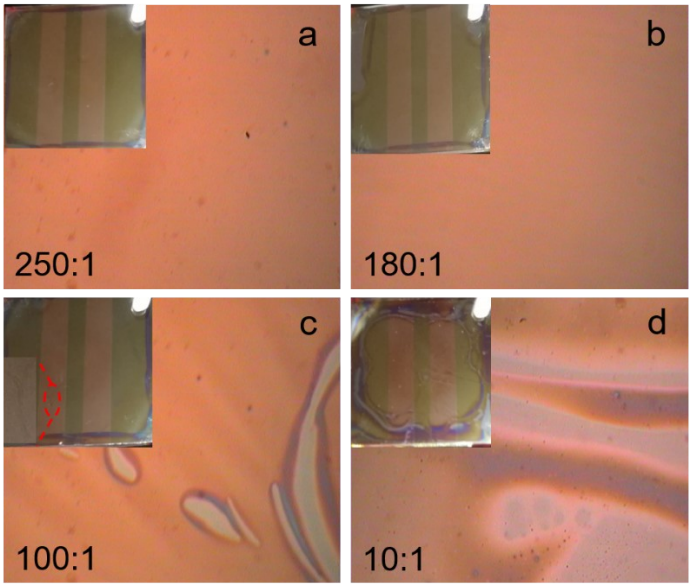

Figure S11. The optical micrographs and the corresponding photograph of ZnO NPs films with different EA-doping ratios spin-coated on the substrate of the multilayer of ITO/PEDOT:PSS/poly-TPD/PVK/QDs. a) 250:1. b) 180:1. c) 100:1. d) 10:1.

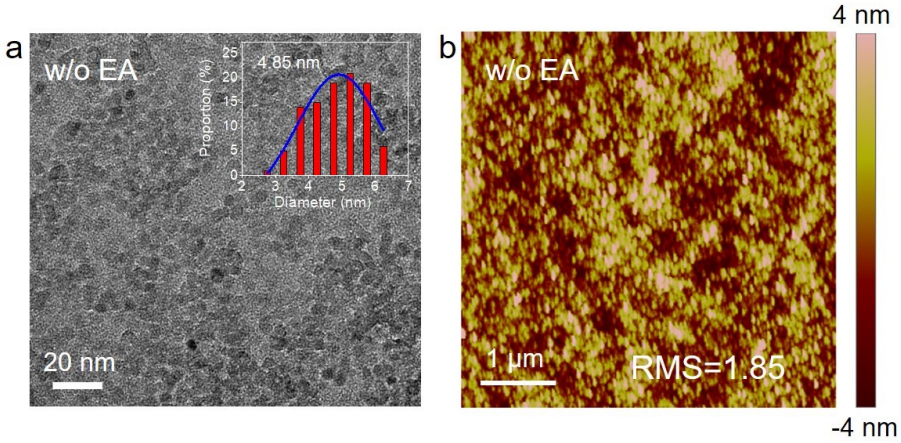

Figure S12. (a) The TEM image of ZnO NPs without EA. (b) The AFM image of ZnO NPs film without EA.